Segmentation of knee cartilage by using a hierarchical active shape model based on multi-resolution transforms in magnetic resonance images

Madeleine León[a], Boris Escalante-Ramirez[b]
[a] Posgrado en Ingeniería Eléctrica, Universidad Nacional Autónoma de México, Mexico City, Mexico.
[b]Departamento de Procesamiento de Señales, Facultad de Ingeniería, Universidad Nacional Autónoma de México, Mexico City, Mexico.

ABSTRACT

Knee osteoarthritis (OA) is characterized by the morphological degeneration of cartilage. Efficient segmentation of cartilage is important for cartilage damage diagnosis and to support therapeutic responses. We present a method for knee cartilage segmentation in magnetic resonance images (MRI). Our method incorporates the Hermite Transform to obtain a hierarchical decomposition of contours which describe knee cartilage shapes. Then, we compute a statistical model of the contour of interest from a set of training images. Thereby, our Hierarchical Active Shape Model (HASM) captures a large range of shape variability even from a small group of training samples, improving segmentation accuracy. The method was trained with a training set of 16- MRI of knee and tested with leave-one-out method.

Keywords: Osteoarthritis, Magnetic resonance images, Hierarchical active shape models, wavelet transform, Hermite transform.

1. INTRODUCTION

The knee is the largest joint in the body, it provides stability and flexibility, allowing the leg to rotate and to stretch. The articular cartilage is a part of the knee and it is a resilient thin material that covers the end of the bones,(i.e., it acts as a kind of cushion to prevent friction between the femur, the tibia and the patella). The cartilage plays a role in shock absorption and it allows the articulation movement.

The cartilage can be altered by mechanical causes such as: shocks, sharp turns, or continuous overloads that may result in various types of injury. The greater the injury, the greater the OA progression risk.

Knee OA is a major cause of impaired mobility affecting more than 10% of general population[1], mainly in people aged above 60 years [2-4]. With increasing age and obesity, it is expected to become a major disabling disease in the future[1].

Currently, the treatment of OA is mainly restricted to control symptoms[5]. Several pharmacologic drugs retarding or inhibiting the progression of structural changes on joint tissues are still in development. In this context, the quantitative evaluation of the cartilage damage is important for monitoring the progression of this disease and for evaluating therapeutic responses[6]. A major step to obtain such quantitative measures is the efficient cartilage segmentation.

The most common method to assess knee cartilage segmentation is to use manual segmentation by an expert; nevertheless, it is prone to variability of observer perception. It is thus advantageous to automatize the segmentation method. The main challenges in developing an automatic method are the thin structure of cartilage and the low contrast between the cartilage and surrounding soft tissues[5].

MRI is the leading image modality for direct non-invasive assessment of the articular cartilage[7]. Cartilage deterioration can be detected using quantitative MRI analysis[8].

If the precise cartilage location is known and regular shape is assumed in most images of knee cartilage, techniques based on prior knowledge can be efficiently applied. Recently, Fripp[9] described an automatic cartilage segmentation system based on the deformation of a statistic shape by using Active Shape Model (ASM) with *a priori* knowledge. ASM was proposed by Cootes[10], this method is used to localize the object of interest on the image. Generally, principal component analysis (PCA) is used to capture main variation modes within a given training set. However, it has two

IX International Seminar on Medical Information Processing and Analysis, edited by Jorge Brieva, Boris Escalante-Ramírez, Proc. of SPIE Vol. 8922, 892214 · © 2013 SPIE · CCC code: 0277-786X/13/$18 · doi: 10.1117/12.2035534

major limitations: First, it often restricts the deformable shape, particularly if it has been trained on a relatively small number of samples, since the number of principal components extracted from the diagonal of the covariance matrix is limited by the number of training shapes[21]. Second, eigenvectors of the covariance matrix encode the most global variation modes in the shapes[21].

Hence, we use the Hermite transform as an additional multi-scale representation method to the wavelets proposed by Davatzikos[11-12]. Davatzikos proposed a multi-scale shape using 1-D wavelet to produce a scale space decomposition of the signal[13]; coefficients are grouped into bands using a logarithm tree to divide the space-frequency domain. The eigenvectors corresponding to bands at coarse scales reflects global shape characteristics, whereas the eigenvectors corresponding to bands at finer scales reflect local shape characteristics at a particular segment of the curve[14]. The authors show that this segmentation technique which uses multi-resolution transforms is more accurate than the segmentation with traditional active shape models[14]. They proved this method on corpus callosum images and they obtained convincing results. They also show that their method has better results than classical ASM when the training set has few images. This paper is organized as follows: wavelets transform and the Hermite transform are described in section 2; section 3 illustrates the methodology implemented. In section 4 and 5 showed the results and conclusions of the project.

2. MULTI-RESOLUTION TRANSFORM

2.1. Hermite Transform

The Hermite Transform (HT), formally introduced by Martens[19-20] to the area of digital image processing, is a multi-scale technique that uses a Gaussian window as a function analysis (see Figure 3). The one dimensional analysis functions of the Hermite transform of degree *n* can be written as:

$$D_n(x) = \frac{(-1)^n}{\sqrt{2^n n!}} \cdot \frac{1}{\sigma\sqrt{\pi}} H_n\left(\frac{x}{\sigma}\right) e^{-\frac{x^2}{\sigma^2}}$$

$$H_n(x) = (-1)^n e^{x^2} \frac{d^n e^{-x^2}}{dx^n}, \qquad n = 0,1,2, \ldots, \tag{1}$$

where $H_n(x)$ are the Hermite polynomials given by the Rodrigues' formula, and d^n/dx^n is referred to the n-th derivate of the Gaussian function (Figure 3).
The Hermite transform applied in the *x* and *y* coordinates directions of the contours in ASM, before applying PCA. The contour coordinates are treated separately as functions 1-D. We have the points set X of $Nx2$ dimension:

$$X = \begin{bmatrix} x_1 & y_1 \\ x_2 & y_2 \\ \vdots & \vdots \\ x_N & y_N \end{bmatrix} \tag{2}$$

The columns are divided in two sets of $Nx1$ dimension, getting the *x* and *y* coordinates separately.

$$X\_1D = \begin{bmatrix} x_1 \\ x_2 \\ \vdots \\ x_N \end{bmatrix} \qquad Y\_1D = \begin{bmatrix} y_1 \\ y_2 \\ \vdots \\ y_N \end{bmatrix} \tag{3}$$

Hermite transform is applied to X_1D and Y_1D.

2.2. Decomposition Using Wavelet Transform:

A wavelet is a waveform of limited duration. The wavelet transform decomposes the original signal into scaled and translated versions of a predefined mother wavelet[15]. The original signal is first divided into two bands of low and high scale contents. These representations are known as the approximation (coarse scale) and the detail (fine scale). The approximation is then further divided into low and high scale bands, and the process is repeated a suitable number of times. This yields a hierarchy of coefficients organized in a tree structure according to scale and location, as shown in Figure 1.

We applied the wavelet transform to the contour coordinates as shown in section 2.1, obtaining its wavelet coefficients[11]:

$$c_n = W(X\_1D_n) = [c_{n,i,} i = 1,..L]\,, \quad d_n = W(Y\_1D_n) = [d_{n,i,} i = 1,..L], \quad (4)$$

where W (.) denotes th wavelet decomposition, the index i is related to the spatial location along the contour, around which the shape information is collected[10].
The two resulting wavelet coordinate vectors are concatenated into a single observation (see equation 5.) to apply PCA. This process is repeated for all shapes in the dataset.

$$W_n = [c_{n1}, d_{n1}, c_{n2}, d_{n2}, \dots, c_{nL}, d_{nL}]^T \quad (5)$$

The complete statistical shape model includes the mean and covariance matrix of the wavelet coefficients for each band[16]. The eigenvectors and eigenvalues of the first few bands generally represent aspects of shape variability, bands with higher indices[11].

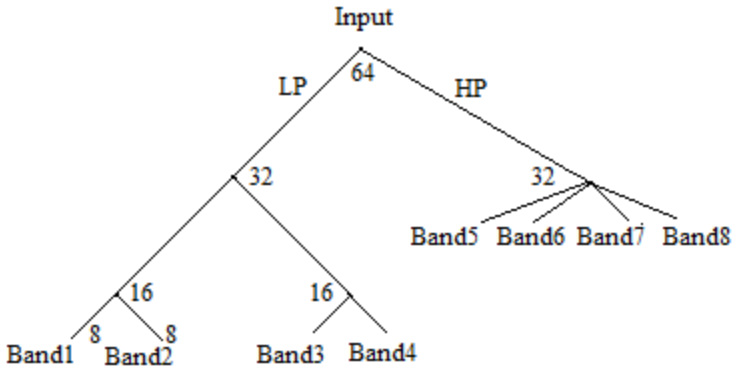

Figure 1. Hierarchical representation of a wavelet transform. Leftmost branch represents approximations, while the rest of the branches correspond to details at different scales.

3. METHODOLOGY

We used a database with 16 training images (384x384 pixels), acquired from a magnetic resonator 3T with Mapit-multi-echo sequence. The segmentation method is shown in figure 2. Manual segmentation was performed by marking consecutive 64 points along the contours annotated by an expert.

During the training stage, the sample shapes were used to get a mean shape. We applied multi-resolution transform to coordinates x and y of the aligned contours, the aim is to extract more information from contours at different spatial resolutions. We tested HT and two different wavelets, namely, the Haar and the Sym-5. With these transformed coordinates, we calculate principal components getting eigenvectors and eigenvalues of variation modes.

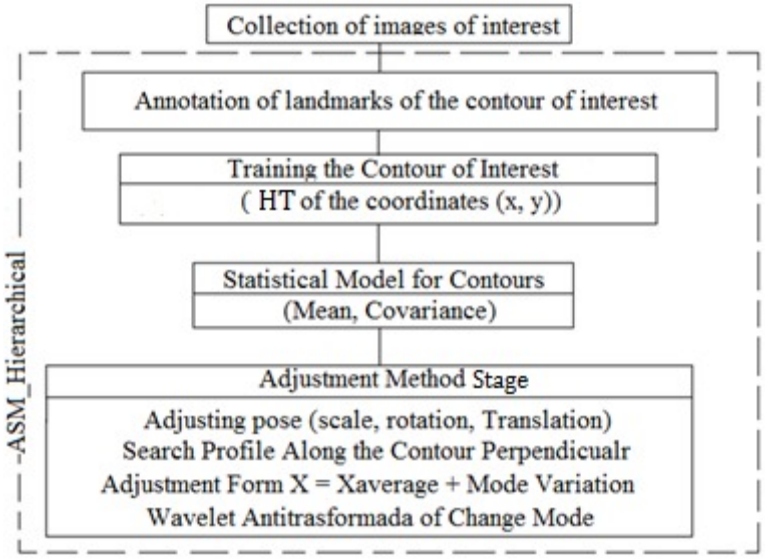

Figure 2. A general diagram of we proposal

This training ends with the acquisition of level gray profiles of the marked contours (robust to intensity changes) and calculation of the covariance matrix.

On the fitting stage (see Figure 2), the first position adjustment in terms of translation, rotation and scale was performed. The landmarks displacements were obtained minimizing the Mahalanobis distance between gray profiles and the mean gray profile calculated on the training stage. The multi-resolution transformation was applied to obtain the variation modes of the new landmark positions. For this implementation, we applied an inverse transform to return to the contour framework.

We applied the HT on the contour coordinates (see equation 3). Our implementation computes up to a sixth Gaussian derivative order (see Figure 3). In wavelets, we used a three-level decomposition tree (see Figure 1). This decomposition starts with 64 marked points on the contour. We obtained eight bands with eight points each one at the end of the transformation. Each band is represented by their global and local components, respectively.

For validation we used the Dice Similarity Coefficient (DSC), it measures the spatial overlap between two segmentations, A and B target regions, and DSC is defined as[17]:

$$DSC(A,B) = 2(A \cap B)/(A + B) \quad (6)$$

Where A is the gold standard segmentation which, in our case, refers to the manual segmentation by an expert, and B is the segmentation mapped from the deformable image. This metric is symmetric and sensitive to differences in both scale and position[18]. The DSC represents the spatial overlap and reproducibility. A *DSC* value of 0 indicates that there is no overlap; a value of 1 indicates perfect overlap. The nearer to 1, the better the overlap.

4. RESULTS

We first tested the standard ASM for different numbers of training samples. In figure 4, we noticed that a number of 16 samples a good segmentation was obtained, the segmentation error increased rapidly when 5 samples were used. We obtained an average *DSC* of: ASM-DSC = 0.8365(for figure 4(a)) and ASM-DSC = 0.6321(figure 4(b)). (See figure 4). In figure 4(b) we note that during the adjustment stage, edge points try to attract the landmark points which can result in failure because the projection moves the contour far away from its desired location.

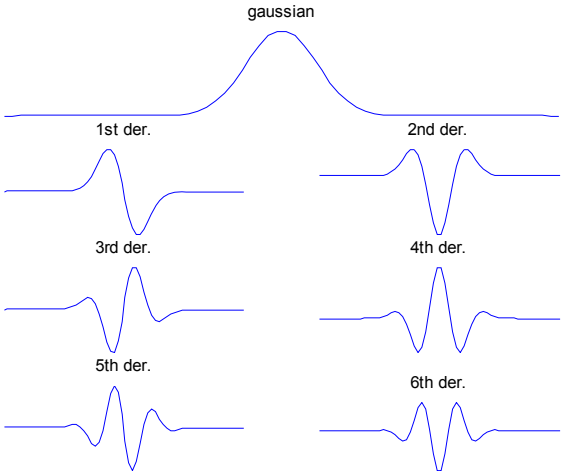

Figure 3. Representation of Hermite functions

It is clear that ASM needs to be trained on a sufficiently large number of samples in order to capture finer details of shapes. When only a very limited number of training samples (5 samples) were available, the standard ASM failed to find the desired contours, because the ASM trained on five samples is too restrictive. This is not the case with hierarchical methods.

(a) (b) (c)

Figure 4. (a) MRI images, (b) ASM with 16 numbers of training samples, (c) ASM with 5 numbers of training samples

For the case of hierarchical methods, testing was conducted with wavelets Haar and Sym5, as well as the Hermite transform, (See figure 5). In order to compare the performance of the different transforms, we used the same initialization and adjustment scheme for all models.

We notice that Sym5 wavelet and Hermite transform deliver the best fitting, with very similar results. The Haar wavelet stands slightly behind.

In Table 1 and figure 6 show the *DSC* average and standard deviation values of the Hierarchical Segmentation with 16 and 5training images.

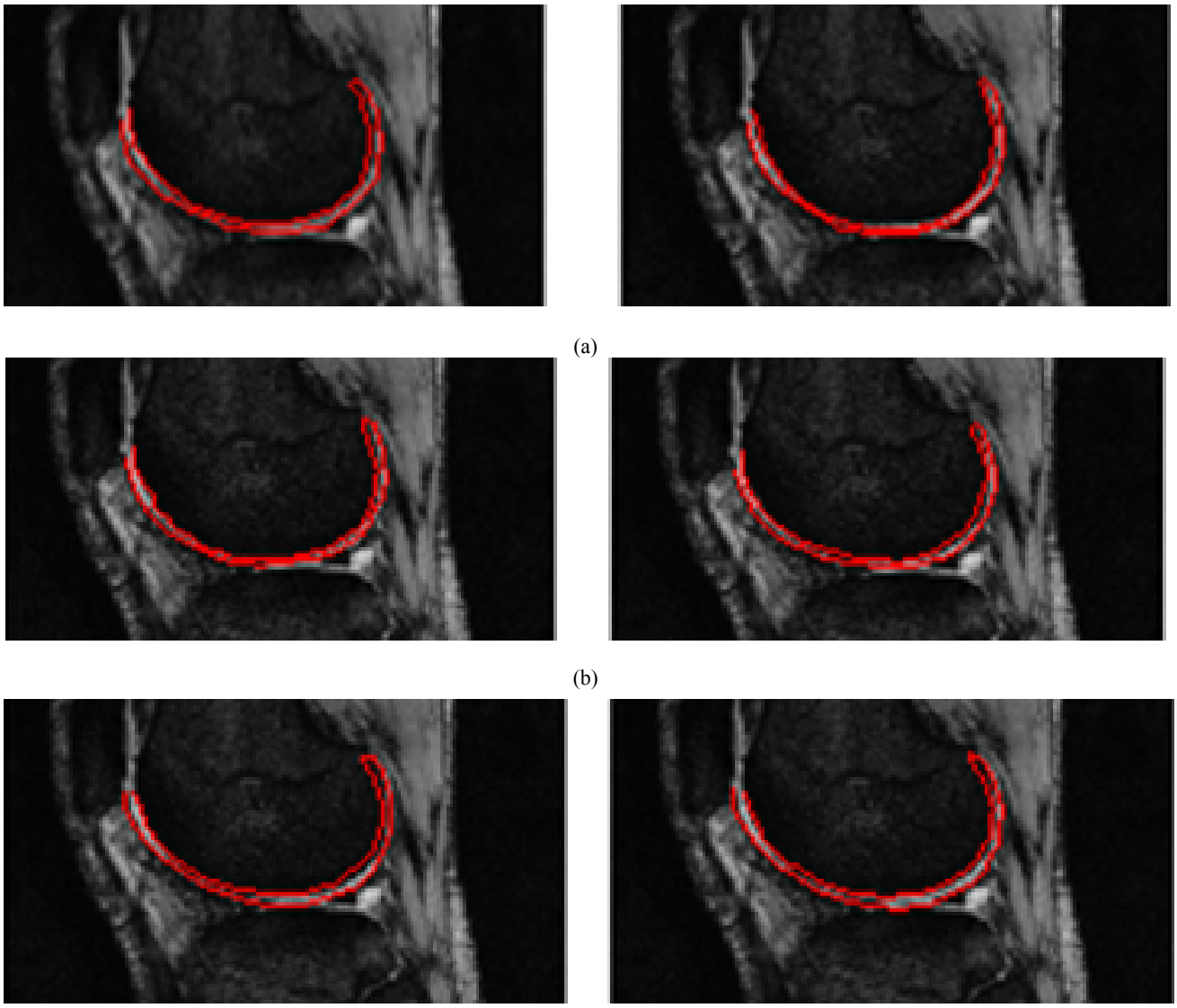

Figure 5. (a) Segmentation of the image with HT, Using total of images (left) and images for training (right).(b) with Sym5-wavelet transform for Using total of images (left) and images for training(right). (c) With Haar-wavelet transform for Using total of images (left) and images for training (right).

Table 1. *DSC* average and deviation standard (STDEV) results using 16 and 5 training samples

Number of training	Average Haar	Average Sym5	Average Hermite	STDEV Haar	STDEV Sym5r	STDEV Hermite
16 images	0.8138	0.8329	0.8236	0.0346	0.0260	0.0260
5 images	0.7850	0.8041	0.7964	0.0676	0.0396	0.0429

We notice that for the case of Hierarchical ASM, five training samples are enough to achieve good and fast results, since this method provides efficient ways to describe global and local information shown in the training samples. In contrast, for the case of standard ASM, details found in only 5 training samples are insufficient to describe global shape variations and they are not reflected in a statistical model. We used leave-one-out validation method for this small image set.

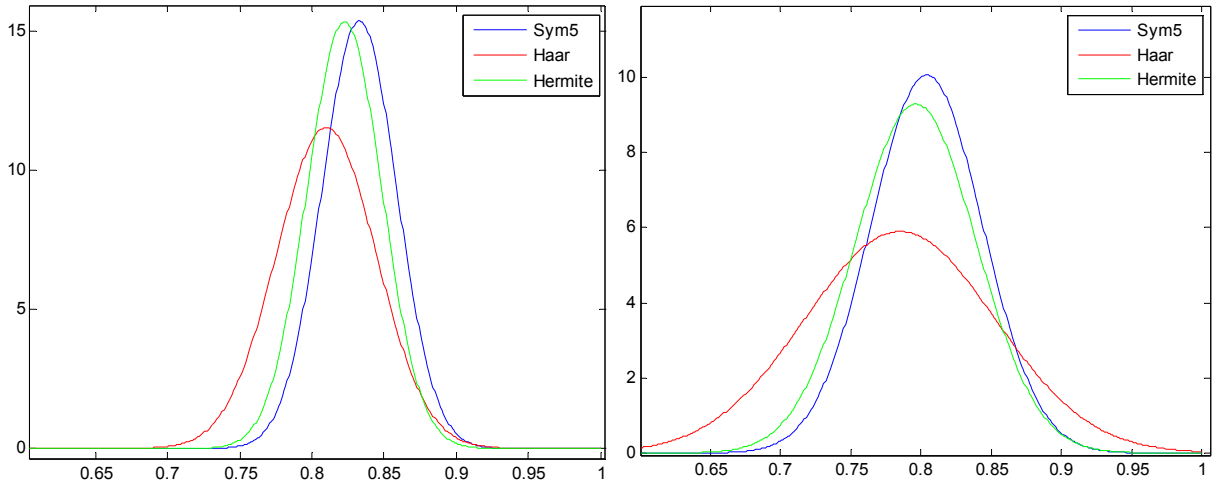

Figure 6. Representation of STDEV with the samples of training (a) 16 samples images, (b) 5 samples images

5. CONCLUSION

In this paper, we presented a hierarchical representation of the contours of knee cartilage using the Hermite Transform and compared it with similar structures using wavelet transforms. The multi-scale nature of the Hermite transform and wavelets allows capturing local and global shape deformations using few training samples.

The hierarchical ASM delivers better results than the standard ASM even in the cases of only 5 training samples to construct the mean shape and to obtain statistical parameters.

Obtaining a large number of training medical images is often very difficult. For this reason, having a good segmentation method that needs few training samples is very useful in medical image processing. Future work, may improve segmentation performance by proposing alternative fitting methods of ASM, and changing the shape description. A stop criterion may be included in the iterative adjustment to accelerate segmentation process.

ACKNOWLEDGMENT

The authors greatly acknowledge the support of research grants from UNAM PAPIIT IN113611 and CONACYT-333500

REFERENCES

[1] A. D. Woolf and B. Pfleger, "Burden of major musculoskeletal conditions," *Bulletin of the World Health Organization*, vol. 81, pp. 646 – 656, 09 2003.

[2] D. Jackson, T. Simon, and H. Aberman, "Symptomatic articular cartilage degeneration: The impact of the new millenium," *Clinical Orthopaedics And Related Research*, vol. 391, pp. 14–25, 2001.

[3] E. Bagge, A. Bjelle, S. Ed´en, and A. Svanborg, "Osteoarthritis in the elderly: clinical and radiological findings in 79 and 85 year olds," *Ann Rheum Dis*, vol. 50, no. 8, pp. 535–9, Aug 1991.

[4] C.G. Peterfy, C. F. van Dijke, D. L. Janzen, C. C. Gluer, R. Namba, S Majumdar, P. Lang, H. K. Genant , "Quantification of rticular cartilage in the knee by pulsed saturation and fat-supressed MRI: optimization and validation," Radiology 192 (2), pp.485-491, 1994.

[5] Jenny Folkesson, *Member, IEEE*, Erik B. Dam, Ole F. Olsen, *Member, IEEE*, Paola C. Pettersen, and Claus Christiansen, "Segmenting Articular Cartilage Automatically Using a Voxel Classification Approach", IEEE Trans. Med. Imag., vol. 26, no. 1, January 2007

[6] Pierre Dodin, Jean-Pierre Pelletier, Johanne Martel-Pelletier*, and Franc¸ois Abram, "Automatic Human Knee Cartilage Segmentation From 3-D Magnetic Resonance Images", IEEE Trans. On Biomedical Engineering, Vol. 57, NO. 11, November 2010.
[7] H. Graichen, R. Eisenhart-Rothe, T. Vogl, K.-H. Englmeier, and F. Eckstein, "Quantitative assessment of cartilage status in osteoarthritis by quantitative magnetic resonance imaging," *Arthritis Rheumatism*, vol. 50, no. 3, pp. 811–816, Mar. 2004.
[8] E. Pessis, J.-L. Drape, P. Ravaud, A. Chevrot, and M. D. X. Ayral, "Assessment of progression in knee osteoarthritis: Results of a 1 year study comparing arthroscopy and mri," *Osteoarthritis Cartilage*, vol. 11, pp. 361–369, 2003.
[9] J. Fripp, S. Crozier, S. K. Warfield, and S. Ourselin, "Automatic segmentation of articular cartilage in magnetic resonance images of the knee," *Int. Conf. Med. Image Comput. Assist. Interv.*, vol. 10, pp. 186–194, 2007.
[10] T. Cootes, C. Taylor, D. Cooper, J. Graham, "Active shape mdels their training and application," Computer Vision and Image Understanding, 61(1), pp. 38-59, 1995.
[11] C. Davatzikos, X. Tao, D. Shen, " Hierarchical Active Shape Models, Using the Wavelet Transform," IEEE Trans. on Medical Imaging, vol. 22(3), 2003.
[12] A. Mohamed, C. Davatzikos, " Shape Representation via Best Orthogonal Basis Selection," MICCA 2004, Lecture Notes in Computer Science, Springer-Verlag, pp. 225-233, 2004.
[13] Mallat, S. (1999). "A wavelet tour of signal processing". Access Online via Elsevier. (1999)
[14] Sjostrand, K., Rostrup, E., Ryberg, C., Larsen, R., Studholme, C., Baezner, H.,& Waldemar, G. "Sparse decomposition and modeling of anatomical shape variation". *Medical Imaging, IEEE Transactions on*, *26*(12), 1625-1635. (2007).
[15] I. Daubechies and Y. Meyer, "Ten lectures on wavelets," *Bull. Am. Math. Soc.*, vol. 28, no. 2, pp. 350–359, 1993.
[16] Davatzikos, C., Tao, X., & Shen, D. " Applications of wavelets in morphometric analysis of medical images". *SPIE Wavelets X, San Diego, CA*. (2003).
[17] Zou, K. H., Warfield, S. K., Bharatha, A., Tempany, C., Kaus, M. R., Haker, S. J., & Kikinis, R. "Statistical validation of image segmentation quality based on a spatial", scientific reports. Academic radiology, *11*(2), 178-189 (2004).
[18] Varadhan, R., Karangelis, G., Krishnan, K., & Hui, S. "A framework for deformable image registration validation in radiotherapy clinical applications". Journal of Applied Clinical Medical Physics, *14*(1), (2013).
[19] Martens, J.-B. "The hermite transform-applications". IEEE Transactions on Acoustics, Speech and Signal Processing 38, 9 (1990), 1607–1618.
[20] Martens, J.-B. "The hermite transform-theory". IEEE Transactions on Acoustics, Speech and Signal Processing 38, 9 (1990), 1595–1606.
[21] Nain, D., Haker, S., Bobick, A., & Tannenbaum, A. (2007). Multiscale 3-d shape representation and segmentation using spherical wavelets. *Medical Imaging, IEEE Transactions on*, *26*(4), 598-618.